JOURNAL OF CATALYSIS 119, 215–229 (1989)

Thermodynamics of H_2 Dissociation into Spilt-over Hydrogen over Pt/Transition Metal Oxide Systems

XUEHAO LIN, J. F. LAMBERT, J. J. FRIPIAT, AND C. ANCION*

*Department of Chemistry and Laboratory for Surface Studies, University of Wisconsin-Milwaukee, P.O. Box 413, Milwaukee, Wisconsin 53201, and *Group de Physico-Chimie Minerale et de Catalyse, 1 Place Croix du Sud, Louvain la Neuve B-1348, Belgium*

Received December 30, 1988; revised May 23, 1989

The isotherm and enthalpy $\Delta\overline{H}_{ir}(H_2)$ of the intercalation process of molecular H_2 into $VMoO_{5.5}$ coated with 1% Pt leading to the formation of the $H_xVMoO_{5.5}$ hydrogen bronze have been measured. Up to $x = 2.85$, the hydrogen uptake is mediated by hydrogen spillover and $\Delta\overline{H}_{ir}(H_2) = -30.5$ kcal mol^{-1}. For $2.85 < x < 3.31$, $|\Delta\overline{H}_{ir}|$ is less than 3 kcal mol^{-1}, indicating that H_2 is physisorbed or weakly chemisorbed in microfractures produced within $VMoO_{5.5}$ microcrystals by anisotropic modifications of the lattice parameters due to hydrogen uptake. $\Delta\overline{H}_{ir}(H_2)$ is the sum of two terms, indistinguishable by calorimetry, namely, $\Delta\overline{H}_d(H_2)$ corresponding to the dissociation of H_2 into active spilt-over species (H_s) with partial electron transfer to the lattice and $\Delta\overline{H}_i(H_2)$ which measures the uptake of H_s by the oxide host lattice. $\Delta\overline{H}_i(H_2)$ can be computed separately using a statistical thermodynamics treatment developed recently (Fripiat *et al., J. Phys. Chem.* **93,** 2083 (1989)) applied to the intercalation isotherm. Therefore, $\Delta\overline{H}_d$ (which should not be confused with the heat of dissociative chemisorption on Pt) can be computed from $\Delta\overline{H}_{ir}(H_2) - \Delta\overline{H}_i(H_2)$. When compared with previous results $\Delta\overline{H}_d(H_2)$, in kilocalories per mole, on Pt, scales as follows:

$$-5.26(H_xWO_3) > -11.4(H_xMoO_3) > -16.9(H_xV_2O_5) > -18.2(H_xVMoO_{5.5}).$$

This large spread is tentatively explained in terms of the variation of the Fermi level of the metal, pinned upon the Fermi level of the bronze, with respect to the Fermi level of the metal on the unmodified oxide. $\Delta\overline{H}_d(H_2)$ is independent of the metal particle size.

INTRODUCTION

Intercalation (or insertion) isotherms of hydrogen within transition metal oxides, mediated by hydrogen spillover (*1*) from Pt metal particles and leading to nonstoichiometric hydrogen bronzes are "step" isotherms. When represented as a semilogarithmic plot of the H_2 pressure vs $\alpha = x/x_m$ (x being the H/M ratio), the steepness of the slope near the inflection point, the downward or upward curvature on both sides of this point, and the value of ln $P(H_2)$ at the inflection point are characteristic of each bronze. It has been shown (*2*) that experimental isotherms can be fitted with theoretical isotherms in which the average enthalpy is the weighted sum of the energy of occupied (E_o), prevented (E_p), and vacant (E_v) sites and in which the entropy term corresponds to the number of configurations of occupied, prevented, and vacant sites within an idealized network of interstitial sites. The neighboring relationship within this "interstitial lattice" can be represented by a Z-regular graph, Z being the number of neighbors of any interstitial site. Filling the interstitial lattice (thus increasing the statistical probability, X_o, of any site being occupied) is assumed to obey the single constraint that the occupation of one site prevents the Z neighboring sites from being occupied. The probability (X_p) of a site being prevented has been obtained by computer simulation and a simple analytical relationship has been found to approximate the dependency of X_p to X_o. Each model of "interstitial lattice" is characterized by a parameter $\zeta = ZX_{om}/(1 - X_{om})$ where X_{om} is the maximum fractional occu-

0021-9517/89 $3.00

pation probability. X_{om}, also obtained from the simulation procedure, is related to the departure from stoichiometry in the hydrogen content.

Fitting the experimental and theoretical isotherms permits the calculation of the actual intercalation enthalpy, and from the difference between this enthalpy and the experimental enthalpy (obtained through calorimetric measurement), the enthalpy of dissociation of H_2 on the supported metal into spilt-over hydrogen is obtained. Significant changes observed are evident in the dissociation enthalpy, depending on the nature of the bronzes, indicative of the differences in affinity for electron transfer to the oxide lattices as well as of different interactions with the supported metal.

The intercalation enthalpy ($\Delta\overline{H}_i(H_2)$) and the dissociation enthalpy $\Delta\overline{H}_d(H_2)$ obtained for the three bronzes studied so far are reported in Table 1.

The present contribution aims to extend the approach suggested in Ref. (*2*) to the bronze of a mixed oxide $VMoO_{5.5}$ which presents several interesting properties. $VMoO_{5.5}$ and its bronze $H_{3.3}VMoO_{5.5}$ are orthorhombic (*3*); the intercalation of hydrogen increases the *a* and *b* unit cell parameters and decreases the *c* parameter as follows:

$$\Delta a/a = 4.85\%,\ \Delta b/b = 2.89\%,$$
$$\text{and } \Delta c/c = -6.98\%.$$

The crystallinity is not affected in a cycle of oxidation (in the presence of O_2) and reintercalation of hydrogen after oxidation as shown in Fig. 1 (from Ref. (*4*) and references therein). Up to about 20% of the maximum H content can be removed reversibly at 60°C upon outgassing $H_{3.3}VMoO_{5.5}$, while the depletion of the initial H content is only about 5% in $H_{1.7}MoO_3$ at 30°C and in $H_{3.6}V_2O_5$ at 120°C. Thus, hydrogen is apparently more easily deintercalated from $H_{3.3}VMoO_{5.5}$ than from the "parent" MoO_3 and V_2O_5 bronzes. In this work we report a large number of calorimetric measurements dealing with hydrogen intercalation in, and deintercalation from, $H_{3.3}VMoO_{5.5}$ coated with small metal Pt particles. The heat of the oxidation reaction (with molecular O_2) and the heat of reintercalation after oxidation have been measured as well.

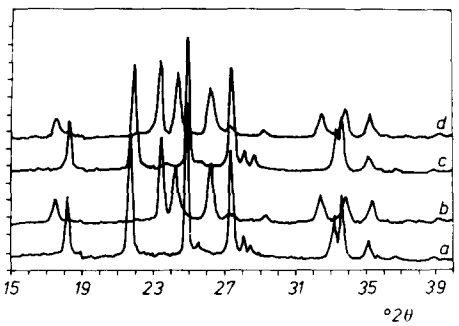

FIG. 1. Reversibility of H intercalation reaction. XRD patterns (Cu$K\alpha$): (a) initial $VMoO_{5.5}$; (b) $H_{3.3}VMoO_{5.5}$; (c) the same oxidized at 120°C for 3 hr in O_2; (d) the same reexposed for 5 min to H_2 (200 Torr) at 60°C. The Pt content was 1% (w/w).

From these data $\Delta H_{ir}(H_2)$ of the intercalation reaction is obtained:

$$\Delta\overline{H}_{ir}(H_2) = \Delta\overline{H}_i(H_2) + \Delta\overline{H}_d(H_2).$$

Then from an accurate intercalation isotherm $\Delta\overline{H}_i$ is calculated using the theory explained in Ref. (*2*) and recalled above. $\Delta\overline{H}_d(H_2)$ is obtained and compared with the values shown in Table 1.

Calorimetric as well as stoichiometric data are most easily explained in terms of the existence of two distinct populations of

TABLE 1

Values Obtained for $\Delta\overline{H}_i(H_2)$ and $\Delta\overline{H}_d(H_2)$ in $H_{0.4}WO_3$, $H_{1.7}MoO_3$, and $H_4V_2O_5$

Bronze	$-\Delta\overline{H}_i(H_2)$	$-\Delta\overline{H}_d(H_2)$	T(K)	$-\Delta\overline{H}_{ir}(H_2)$
$H_{0.4}WO_3$	11.2	5.3	373	16.5
$H_{1.7}MoO_3$	13.6	11.4	333	25.0
$H_4V_2O_5$	12.2	16.9	343	29.1

Note. $\Delta\overline{H}_{ir}(H_2)$ is the enthalpy of the intercalation reaction: $\Delta\overline{H}_{ir}(H_2) = \Delta\overline{H}_i(H_2) + \Delta\overline{H}_d(H_2)$, all expressed in kcal mol^{-1}. From Ref. (*2*).

hydrogen. The relative extents of these populations are estimated.

In parallel the influence of the dispersion of the Pt particles has been studied. As could have been anticipated, the degree of dispersion does not influence $\Delta\overline{H}_{ir}(H_2)$; however, the rate processes are strongly dependent upon the Pt dispersion. This kinetics aspect will be described in a separate publication (*5*); in most experiments reported here, the average platinum particle diameter was between 20 and 25 Å.

In summary, this contribution emphasizes the effect of electronic structure, and of the modification of metal–support interaction on molecular H_2 dissociation leading to the formation of hydrogen bronzes in the particular case of Pt on $H_xVMoO_{5.5}$.

EXPERIMENTAL

Material

$VMoO_{5.5}$ was prepared according to the procedure described by Ancion *et al.* (*4, 6*) and its crystallinity was checked by comparing the powder XRD with that of spectrum a, Fig. 1. The powdered oxide was impregnated with 1% Pt (w/w) using either H_2PtCl_6, $Pt(NH_3)_4Cl_2$ or $Pt(NH_3)_4(OH)_2$ as precursors. The platinum salt was decomposed by heating between 200 and 400°C in air or under vacuum. The impregnation and decomposition procedures strongly affect the kinetics of H_2 uptake as described and discussed elsewhere (*5*). In particular, the decomposition of the platinum amine salt requires a temperature >300°C to obtain rapid uptake (total reaction time on the order of 6 hr at 60°C). However, the degree of dispersion of the Pt particles does not significantly affect the thermodynamic results within the margin of experimental errors.

Instruments

The instrumental device is described in Fig. 2. It contains two Seebeck envelope calorimeters manufactured by Thermonetics Corp., San Diego, California. All the heat flow in the calorimeter must pass through its wall where the temperature gradient sensors are located. Therefore, the calorimeter envelope integrates the total heat flow in the system with respect to time. Thermoelectric transducers relate

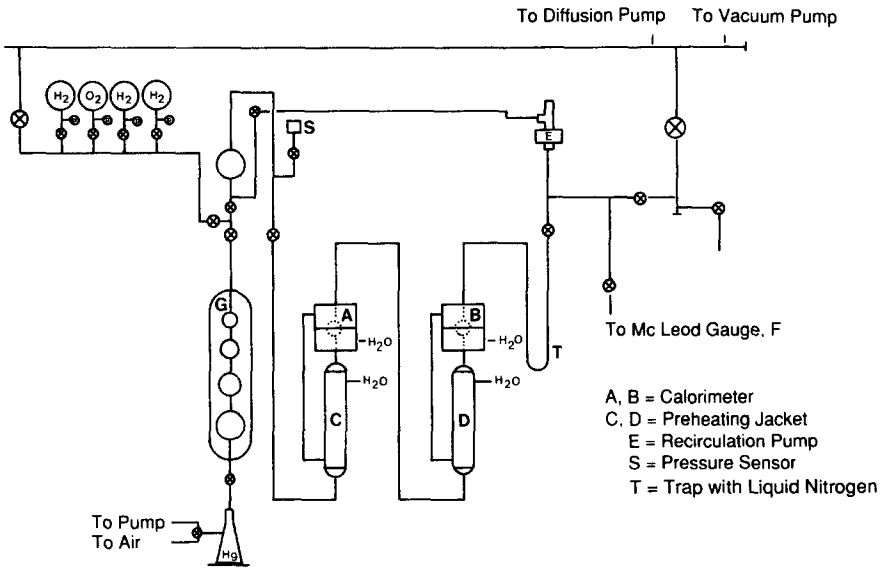

FIG. 2. Apparatus used for determining the integral heats of intercalation and deintercalation of hydrogen as well as the heat of oxidation of hydrogen bronzes and the intercalation isotherm (see text).

thermal flow to a DC voltage output signal which is recorded vs time. The calorimeter envelope is quite thin so that the time constant is low. The transducers consist of thermopiles with spaced junctions. The sensitivity is about 0.01 cal/sec mV. The calorimeters include an environmental control jacket, in which a fluid is circulated at the desired reaction temperature. The reaction vessel is a spherical thin glass container fitted with a sintered glass disk on which about 0.6 g of material is loosely packed. Calorimeters (A and B) contain equal weights of materials either uncoated or coated with Pt particles. The reference is uncoated $VMoO_{5.5}$ which does not react with molecular H_2. The DC signals from both calorimeters are opposed and the difference is recorded. The heating water flow is evenly distributed between the control jackets of the two calorimeters and the preheating jackets (C and D).

A circulation pump transfers the molecular H_2 from (E) into the calorimetric system. The pressure is monitored by pressure sensors (Barocel) and recorded during the reaction. Low pressures are checked with a McLeod gauge (F). A gas buret (G) permits the measurement of the initial amount of H_2 as well as the measurement of the dead volume of the reaction system. A conventional vacuum system (residual pressure $\simeq 10^{-6}$ Torr) is used to outgas the system. Therefore, intercalation isotherms and heat consumed or produced during intercalation, deintercalation, and O_2 oxidation of the bronze can be measured, as well as the kinetics of the intercalation and oxidation reaction.

In this paper all thermodynamic measurements were obtained at 60 ± 0.5°C (333 K). The intercalation isotherms were obtained between 333 and 347 K.

Experiments

Two types of experiments were carried out. In the first type (referred to as one-step procedure) the initial pressure of 200 Torr was large enough to reach, in one step, a final stoichiometry near that of the maximum uptake. In the second type (multi-step procedure) the initial pressure was reduced in order to follow step by step the uptake between $x = 0$ and $x = N_m$, namely, the maximum H/(V + Mo) ratio. In the first case, the integral heat of the intercalation $\Delta\overline{H}_{ir}(N_m)$ was produced in one step. In the second case, $\Delta\overline{H}_{ir}(x)$ was obtained by summing up the heats evolved after each step: $x_1 + x_2 + x_3 + \cdots = x$. Irrespective of how N_m was reached, partial deintercalation under vacuum was carried out and the endothermic heat effect associated with deintercalation $\Delta\overline{H}_{dr}$ (*d*eintercalation *r*eaction) was measured as well.

Deintercalation was followed by a one-step reintercalation, the enthalpy of which was also measured. At this stage the maximum H content should be restored.

After outgassing, the oxidation reaction was performed, the corresponding enthalpy change being $\Delta\overline{H}_o$, and finally a third reintercalation was carried out. For the sake of clarity Table 2 summarizes the sequence of events in the one-step or multi-step procedure. In all the experiments the temperature was 333 K.

In all intercalation reactions Δx was measured by recording the H_2 pressure change. In the oxidation reaction, the O_2 consumption was recorded as well. Of course, a measurement of $-\Delta x$ in the deintercalation measurement was not possible, since this step was performed by outgassing under vacuum for several hours.

The same N_m value was expected to be reached in the first intercalation of the one-step and multi-step procedure. This assumption is correct within experimental uncertainty (±0.1 on Δx).

As far as the second intercalation (after deintercalcation in either the one-step or multi-step procedure) is concerned, it was assumed that $(N_m - x_r)$ was identical to the amount of hydrogen deintercalated. This identity will be demonstrated later on the basis of the $\Delta\overline{H}_{dr}$ measurements.

As outlined in Table 2, the initial hydro-

TABLE 2

Summary of the Experimental Procedure

	Δx	Enthalpy change
One-step procedure		
1st complete intercalation	$0 \rightarrow N_m$	$\Delta\bar{H}_{ir}(N_m)$
Deintercalation	$N_m \rightarrow x_r$	$\Delta\bar{H}_{dr}(N_m, x_r)$
2nd intercalation	$x_r \rightarrow N_m$	$\Delta\bar{H}_{ir}(x_r, N_m)$
Outgassing H_2	$N_m \rightarrow x_r$	
Oxidation	$x_r \rightarrow x'_r$	$\Delta\bar{H}_o$
Outgassing O_2		
3rd intercalation	$x'_r \rightarrow N'_m$	$\Delta\bar{H}_{ir}(x'_r, N'_m)$
Multi-step procedure		
1st intercalation step	$0 \rightarrow x_1$	$\Delta\bar{H}_{ir}(0, x_1)$
2nd intercalation step	$x_1 \rightarrow x_2$	$\Delta\bar{H}_{ir}(0, x_2)$
.	. .	
.	. .	
nth intercalation step	$x_n \rightarrow N_m$	$\Delta\bar{H}_{ir}(N_m)$
Deintercalation	$N_m \rightarrow x_r$	$\Delta\bar{H}_{dr}(N_m, x_r)$
2nd intercalation	$x_r \rightarrow N_m$	$\Delta\bar{H}_{ir}(x_r, N_m)$
Outgassing H_2	$N_m \rightarrow x_r$	
Oxidation	$x_r \rightarrow x'_r$	$\Delta\bar{H}_o$
Outgassing O_2		
3rd multi-step intercalation	$x'_r \rightarrow x'_1$	$\Delta\bar{H}_{ir}(x'_r, x'_1)$
.	$x'_1 \rightarrow x'_2$	$\Delta\bar{H}_{ir}(x'_1, x'_2)$
.	. .	
.	. .	
	$x'_n \rightarrow N'_m$	$\Delta\bar{H}_{ir}(x'_n, N'_m)$

gen content before oxidation is not N_m but x_r, because the sample is outgassed between the second intercalation and the oxidation step. Thus, the O_2 consumption is $(x_r - x'_r)/2$. It will be shown that the maximum hydrogen uptake at the third (and final) reintercalation after oxidation (N'_m in Table 2) is always lower than N_m, in spite of the fact that the sample was outgassed at 60°C till the residual pressure was 10^{-5} Torr in most cases.

RESULTS

One-Step Experiments

Thirteen one-step experiments yielded 25 values for $\Delta\bar{H}_{ir}$, including those obtained for the first and second intercalation processes ($T = 333$ K). A regression analysis linking $\Delta\bar{H}_{ir}$ to the corresponding $x/2$ was performed with the following results:

intercept: 11.06 kcal mol^{-1}, standard error: 5.6 kcal;

slope: -37.76 kcal mol^{-1}, standard error: 2.12 kcal;

correlation coefficient: 0.932.

Among these 13 experiments, four were performed with samples impregnated with the H_2PtCl_6 precursor, one with the $Pt(NH_3)_4Cl_2$ precursor, and eight with the $Pt(NH_3)_4(OH)_2$ precursor. No significant difference attributable to either the precursor, or the way thermal activation was carried out, was detectable in the recorded $\Delta\bar{H}_{ir}$, even though large differences in the kinetics of the H uptake were observed (*5*).

Figure 3 shows the linear regression $\Delta\bar{H}_{ir}$ vs $\Delta x/2$ (solid line) and the average values of $\Delta\bar{H}_{ir}$ obtained within $x/2 = 0.05$ intervals. The number of averaged measurements is shown between parentheses. The cluster of

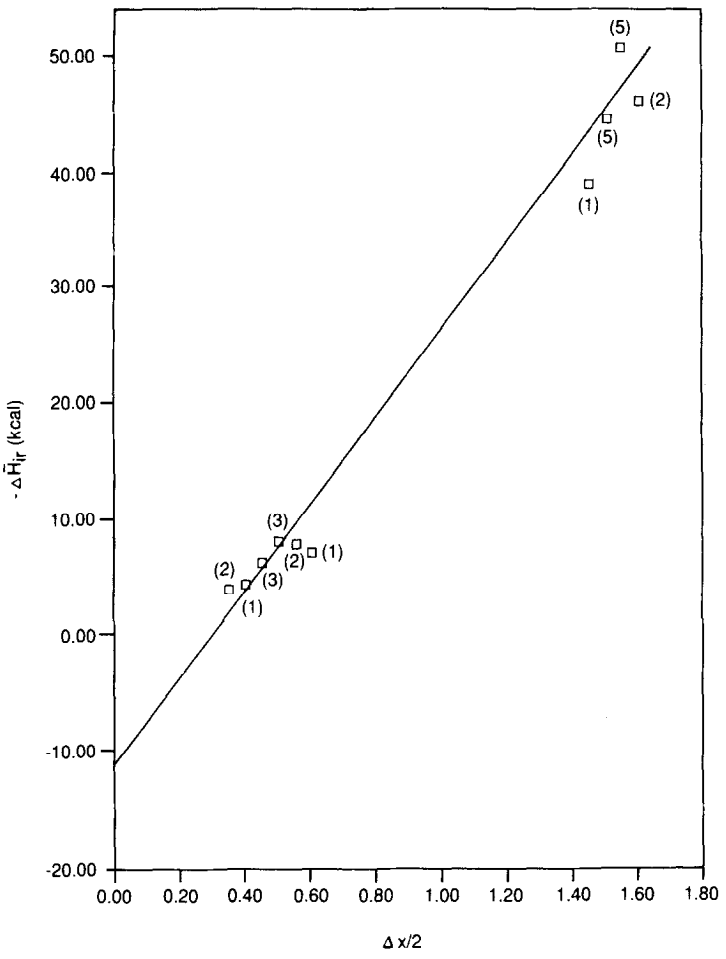

FIG. 3. $-\Delta\overline{H}_{ir}$ vs $\Delta x/2$ in the one-step procedure. Solid line: regression analysis on 25 values. Data points (□): average of (n) experiments within $\Delta x/2 = 0.05$ intervals.

data between $x/2 = 0.25$ and $x/2 = 0.60$ corresponds to the second intercalation (see Table 2). From these data it may be concluded that:

1) $\Delta\overline{H}_{ir}$ per mole H_2 or $\Delta\overline{H}_{ir}(H_2)$ between $x/2 = 0.29$ and 1.6 is -37.8 ± 5.6 kcal mol^{-1}.

2) A fraction $x_f/2 = 0.29$ is intercalated without enthalpy change.

This fraction represents what will be called the "facile" hydrogen. Facile hydrogen may be physisorbed H_2 in fractures created within the $VMoO_{5.5}$ microcrystals, as suggested in the next section.

We may already point out here that desorption measurements support the conclusion that about 0.29 H_2 (per mole oxide) is either strongly physisorbed or weakly chemisorbed as proved by the following measurements carried out on bronzes prepared by a one-step procedure at 60°C. After intercalation and cooling the samples at 20°C, the H_2 pressure in the adsorption apparatus was lowered to about 0.1 Torr, the connection with the vacuum pump was interrupted, and the temperature was raised above 60°C. Hydrogen and water desorption were measured and converted to $\frac{1}{2}\Delta x(H_2)$ and $y(H_2O)$ per mole oxide. The

results were as follows:

T(°C)	120	150	180	200
$\frac{1}{2}\Delta x$	0.22	0.29	0.24	0.03
y	0.02	0.05	0.19	0.44

Thus, up to about 150°C facile H_2 is desorbed while the formation of water is low. Above 150°C the mixed oxide starts reducing under the action of gaseous H_2 and/or intercalated H.

Note that the final equilibrium pressure $P(H_2)$ for which $x = N_m$ was between 135 and 164 Torr in these one-step experiments. Under these conditions N_m was 3.2.

Multi-Step Experiments

Three experiments were performed, the total number of steps $x = 0 \rightarrow x_1 \rightarrow x_2 \cdots \rightarrow x = N_m$ being 23. This includes the multi-step procedure for the first and the third intercalation (after the oxidation and outgassing). The equilibrium pressures vary between 2×10^{-2} and 348 Torr; the maximum hydrogen uptake at the end of the first multi-step intercalation is $N_m = 3.46$, whereas it is $N'_m \leq 2.9$ at the end of the third multi-step intercalation.

The regression analysis performed with the 18 values between $x = 0$ and $x \leq 2.90$ gave the following results:

intercept: -3.02 kcal mol^{-1}, standard error: 3.3 kcal;

slope: -30.53 kcal mol^{-1}, standard error: 1.5 kcal;

correlation coefficient: 0.963.

When x is larger than $2.9 = N_m - x_f$, the $\Delta\overline{H}_{ir}$ measurements are randomly scattered about -46.9 kcal mol^{-1}. The average values of $\Delta\overline{H}_{ir}$ within $x/2 = 0.05$ intervals and the linear relationship $\Delta\overline{H}_{ir}$ function of $x/2$ are shown in Fig. 4. In Fig. 4, five data points out of 23 were obtained with samples where the Pt precursor was H_2PtCl_6 calcined at 200°C under vacuum. For the others, the precursor was $Pt(NH_3)_4(OH)_2$, calcined at 350°C in air. These two situations are, in fact, those with the lowest and the highest Pt dispersion, respectively (*5*).

From these multi-step experiments it fol-

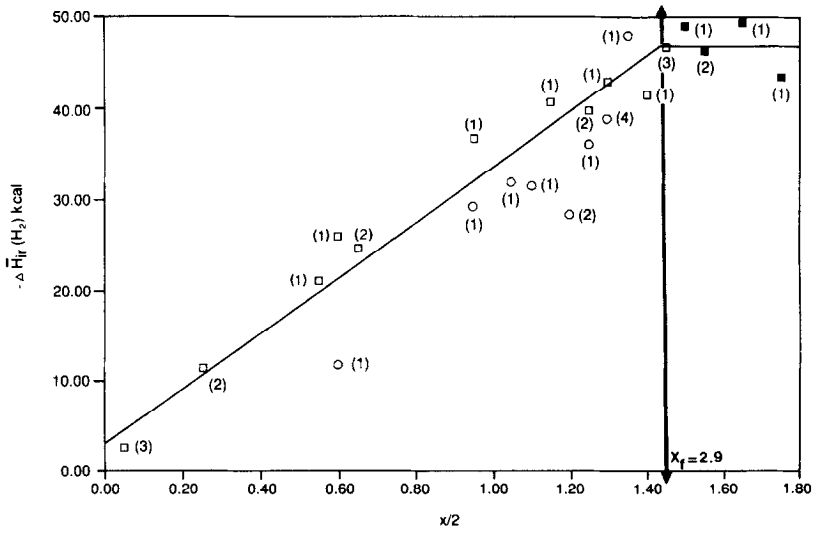

FIG. 4. Multi-step procedure: $-\Delta\overline{H}_{ir}$ vs $x/2$. The arrow indicates the onset of the adsorption of "facile" hydrogen. The squares show the results obtained for the first and third intercalation. The straight line results from the regression analysis on 18 data for $0 < x \leq 2.9$. The squares are obtained for $x > 2.9$. The circles show $\Delta\overline{H}_{ir}$ observed in the third one-step intercalation process for 12 experiments.

lows that $\Delta\overline{H}_{ir}(H_2)$ is -30.5 ± 3.3 kcal mol^{-1}. The standard deviation (from R^2) is lower than that obtained for the one-step experiment. The average $\Delta\overline{H}_{ir}(H_2)$ values obtained with both procedures overlap within the limits of uncertainty. In order to appreciate the margin of error, two points need to be emphasized. First, it may take as long as 6 hr to reach equilibrium, and by the end the recorded heat effect is lost within the noise. More important is the fact that in the one-step experiments were a large exothermic effect is obtained within a few minutes, the local temperature of the sample undergoing intercalation may reach the temperature limit (~150°C) where the bronze becomes unstable, that is, the temperature where water may start forming at the expense of lattice oxygen.

Second, the change in the lattice parameters is abrupt. The volume of the unit cell (*3*) ($a * b * c$) of the oxide is 291.13 Å^3 whereas that of the bronze is 292.15 Å^3. The increase in volume is a moderate 0.38%, but it is very anisotropic, the contraction in the c parameter being on the order of the sum of ($\Delta a/a + \Delta b/b$) expansions. This anisotropic lattice rearrangement is likely to create microfractures within the microcrystals which contribute to increase the N_2 BET surface area (measured after outgassing for 6 hr at 100°C) from 11.3 to 16.2 m^2/g, from the oxide (coated with Pt) to the bronze (after oxidation).

The formation of minute amounts of water, due to overheating in the one-step experiments, could result in overestimating $\Delta\overline{H}_{ir}(H_2)$. This effect must be much less pronounced in the multi-step experiments. Therefore, we suggest that $\Delta\overline{H}_i(H_2) = -30.5 \pm 3.3$ kcal mol^{-1} is nearer the actual enthalpy of intercalation than the value obtained in the one-step experiment. Additional evidence for this choice follows.

Deintercalation

The average experimental $\Delta x = (N_m - x_r)$ during the second intercalation in both the one-step *and* multi-step experiments is 0.94 ± 0.14 where $\sigma = 0.14$ is the standard deviation for 15 data points. Δx should be identical to the H depletion occurring during deintercalation under vacuum.

Using the calorimetric heat of deintercalation $\Delta\overline{H}_{dr}$, the depletion can be estimated in two ways. Either the linear relationship obtained from the one-step experiment, namely,

$$\Delta\overline{H}_{ir} = +11.06 \text{ kcal} - 37.8 \text{ kcal} \cdot \Delta x/2 = -\Delta\overline{H}_{dr} \cdot \Delta x/2, \quad (1)$$

is used or Δx is calculated from

$$\Delta x = -2(\Delta\overline{H}_{dr})/\Delta\overline{H}_{ir}(H_2) + x_f, \quad (2)$$

where $\Delta\overline{H}_{ir}(H_2)$ is -30.5 kcal mol^{-1}, i.e., the value obtained from the multi-step experiment and where $x_f = 0.58$.

The average Δx obtained for 15 measurements of $\Delta\overline{H}_{dr}(H_2)$ is 0.79 ± 0.07 using Eq. (1), whereas that obtained using Eq. (2) is 0.88 ± 0.07. When compared with the experimental $\Delta x = 0.94 \pm 0.14$, it appears that $\Delta\overline{H}_{ir}(H_2) = -30.5$ kcal mol^{-1} is the better estimate.

Therefore, the average stoichiometry of the bronze after prolonged outgassing at 60°C should be $x_r \geq 2.4 \pm 0.1$ H per mole oxide.

Oxidation Reaction

After the second reintercalation, the bronze is outgassed again under similar conditions as those used for the deintercalation step. We can, therefore, expect that at least 2.4 ± 0.1 H atoms remain in the solid before oxidation. In seven out of 10 experiments there is an acceptable agreement in the balance of H consumed by oxidation and H reintercalated as shown in Table 3. In the other three experiments, the oxygen consumption was in excess, perhaps because of incomplete outgassing before oxidation. In this table the measured O_2 consumption is transformed into H consumed: this is the experimental ($x_r - x_r'$) and since x_r is assumed to be 2.4 ± 0.1, x_r' must be about zero; i.e., all the residual hy-

TABLE 3

H Content Balance in the Oxidation Process and Third and Final Reintercalation

Experiment no.	$x(O_2)$ consumed /mole oxide (exp.)	$x_r - x'_r$ H consumed by oxidation (exp.)	$N_m - x'_r$ H reintercalated after oxidation (exp.)	$\Delta\overline{H}_o(H_2)$ or $\Delta H_o(O)$ (kcal/mole H_2O or/oxygen atom)
12	0.654	2.616	2.6	−47.8
15	0.637	2.548	2.64	−40.5
6	0.680	2.72	2.6	−40.7
3	0.759	3.036	2.6	−41.5
2	0.472	1.888	2.6	−46.1
11	0.662	2.648	2.5	−39.4
28	0.788	3.152	2.2	−33.2
Average		2.66 ± 0.26	2.54 ± 0.1	−41.3 ± 8

Note. For the significance of x_r, x'_r and N_m, refer to Table 2.

drogen is consumed during oxidation. The slight excess in oxygen consumption may be due to oxygen chemisorbed on vacancies or other defects within the fractures. The enthalpy $\Delta\overline{H}_o$ for the oxidation reaction is expressed per number of O atoms or H_2 molecules consumed. In other words, it is the integral heat of oxidation divided by $(x_r - x'_r)/2$. The average value is −41.3 ± 8 kcal. The predicted value should be

$$\Delta\overline{H}_o(\text{per } \tfrac{1}{2}O_2) = -\Delta\overline{H}_{ir}(H_2) + \Delta\overline{H}(H_2O), \quad (3)$$

where the enthalpy of formation of liquid water, e.g., −68.3 kcal mol^{-1}, is used without correcting for the fact that the reaction is carried out at 333 K. Thus,

$$\Delta\overline{H}_o = (+30.5 \pm 3.3 - 68.3) \text{ kcal} = -37.8 \pm 3.3 \text{ kcal}.$$

The discrepancy between the predicted and measured value is within the margin of uncertainty. The liquid water must be in some way retained within the host lattice and the microfractures. It should be removed during the outgassing step following oxidation, before the final and third intercalation (see Table 2).

One can wonder why the oxidation process leads to less reproducible results in the measurement of $\Delta\overline{H}_o$ compared with the very reasonable fits shown in Figs. 3 and 4 and/or in the calculation of the H balance (compare for instance the results of Table 3 to $\Delta x = N_m - x_r$ in the deintercalation section). Again, it may be that the sample is overheated by the large thermal effect developed within the few minutes following the introduction of O_2. Since (Table 3) $x_r = 0$, $N_m - x'_r$ should be 3.3 ± 0.1. It is obvious that this is incorrect.

Thus, after oxidation the maximum uptake, N'_m, is *always* smaller than N_m, indicating that the hydrogen intercalation capacity of the host lattice has appreciably deteriorated upon oxidation. Actually, since $N'_m \leq 2.9$ and $N_m \leq 3.465$, one may suggest that the oxidation step has suppressed the sites where facile H_2 was physisorbed. This suggests that strongly physisorbed H_2O molecules within the cracks are not removed upon outgassing at 60°C before the third intercalation.

A previous XRD study of the effect of oxidation has shown (Fig. 6 in Ref. (7)) that when compared to the initial oxide, the intensity of the Bragg reflections of the bronze having reacted with O_2 during 5 min at 120°C is lower than that of the starting oxide, and that the widths of the reflections are appreciably larger (see also Fig. 1c). A

contact time of 20 hr with O_2 at 120°C is necessary to restore the initial XRD pattern of $VMoO_{5.5}$.

It is interesting to point out that the one-step third intercalation also never yields N'_m larger than 2.7 (average hydrogen pressure at equilibrium ~150 Torr), whereas the experimental data shown by empty circles in Fig. 4 indicate that the corresponding $\Delta\bar{H}_{ir}$ (except for two points with $x/2 = 0.6$ and $x/2 = 1.2$) scatter about the linear regression. These one-step third intercalation $\Delta\bar{H}_{ir}$ data were not taken into account in the regression analysis which yields the linear variation in Fig. 4. In contrast, if the one-step third intercalations $\Delta\bar{H}_{ir}$ are compared with the one-step first and second intercalation ΔH_{ir} shown in Fig. 3, it is obvious that they do not follow the linear relationship which holds for samples accepting facile hydrogen.

Additional experiments, such as thermogravimetric measurements during oxidation, are planned in order to obtain information on the removal of water upon outgassing after oxidation.

Intercalation Isotherms

The intercalation isotherm obtained from four different experiments is shown in Fig. 5. What is represented is $\frac{1}{2}\ln(P(H_2)/P^*(H_2))$ vs x, where $P(H_2)$ is the equilibrium pressure corresponding to the uptake of xH atoms and where

$$-\ln P^*(H_2) = \mu_0(H_2)RT = (\bar{F}_0 - E_0^\circ)/RT, \quad (4)$$

$\mu_0(H_2)$ being the reference chemical potential of H_2 obtained from the partition function of gaseous H_2. $(\bar{F}_0 - E_0^\circ)/RT$ is taken from thermodynamic tables (see, for instance, Aston and Fritz (*8*)). Thus, $\frac{1}{2}\ln(P(H_2)/P^*(H_2))$ is $\ln A_g$, where A_g is the absolute activity of the intercalated *guest* hydrogen,

$$RT \ln A_g = \mu_g = \tfrac{1}{2}\mu(H_2), \quad (5)$$

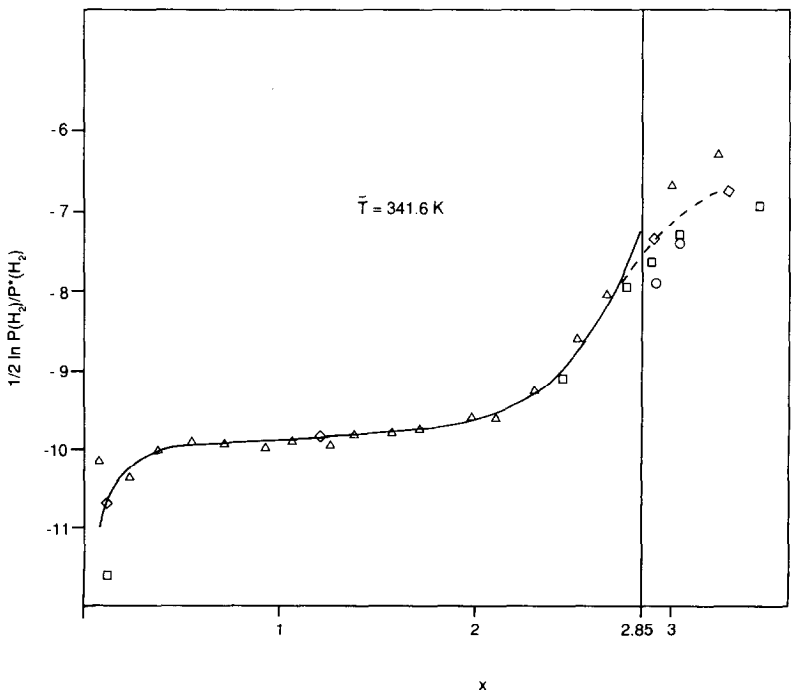

FIG. 5. Intercalation isotherm obtained from four different experiments (□, △, ◇, ○).

and μ_g and $\mu(H_2)$ are the absolute chemical potentials of the intercalated hydrogen and of the gaseous H_2, respectively. Except for the relatively large experimental error in the 0.01 ~ 0.1 Torr range due partially to the very long time necessary to reach equilibrium (>24 hr), the isotherm is smooth up to about $x = 2.85$. In the range between 2.85 and 3.4, namely the range where "facile" hydrogen is taken up without any noticeable enthalpy change (within a margin of uncertainty ±3 kcal), the experimental data are scattered about the dashed line in Fig. 5. It has been suggested earlier that "facile" hydrogen is, in fact, H_2 physically adsorbed or weakly chemisorbed within a network of narrow pores resulting from the anisotropic dilatation of the microcrystals. Therefore, from the isotherm as well as from the calorimetric data we can postulate (1) that the $VMoO_{5.5}$ bronze has the $H_{2.85}VMoO_{5.5}$ stoichiometry, the actual N_m is *not* 3.44 but $(3.44 - x_f) = 2.85$, and (2) that $\Delta H_{ir}(H_2) = -30.5 \pm 3.3$ kcal mol^{-1}.

DISCUSSION

The hydrogen bronze formation can be analyzed, for $0 < x < N_m = 2.85$, as follows:

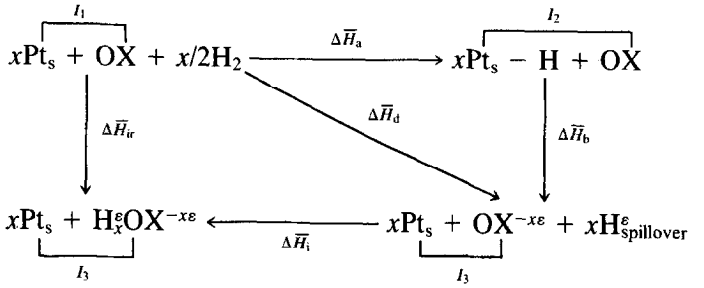

(6)

In the above cycle, Pt_s refers to surface platinum, $H^{\varepsilon}_{spillover}$ to the activated hydrogen spilt over the surface of the oxide, with a partial charge of $+\varepsilon$, OX refers to the original oxide before contact with H_2, and $OX^{-x\varepsilon}$ to the oxide as modified by its interaction with spilt-over hydrogen, which includes the transfer of $x\varepsilon$ electrons. I_1, I_2, and I_3 refer to the interaction enthalpy between the metal and the support, which may be different when either is modified.

In our notation, the overall heat of reaction obtained from the calorimetric experiments is

$$(x/2)\Delta\bar{H}_{ir} = \bar{H}(\mathrm{H}_x^{\varepsilon}\mathrm{OX}^{-x\varepsilon}) - (x/2)\bar{H}(\mathrm{H_2}) - \bar{H}(\mathrm{OX}) + I_3 - I_1. \quad (7)$$

The value $\Delta\bar{H}_i$ corresponds to the intercalation reaction enthalpy

$$(x/2)\Delta\bar{H}_i = \bar{H}(\mathrm{H}_2^{\varepsilon}\mathrm{OX}^{-x\varepsilon}) - \bar{H}(\mathrm{OX}^{-x\varepsilon}) - (x/2)\bar{H}(2\mathrm{H}^{\varepsilon}_{\mathrm{spillover}}). \quad (8)$$

This step, most likely, does not imply a change in the metal–support interaction energy. Thus, the difference $\Delta\bar{H}_d$ between $\Delta\bar{H}_{ir}$ and $\Delta\bar{H}_i$ is

$$(x/2)\Delta\bar{H}_d = [\bar{H}(\mathrm{OX}^{-x\varepsilon}) - \bar{H}(\mathrm{OX})] + (x/2)[\bar{H}(2\mathrm{H}^{\varepsilon}_{\mathrm{spillover}}) - \bar{H}(\mathrm{H_2})] + I_3 - I_1. \quad (9)$$

$\Delta\bar{H}_d$ contains three terms: $[\bar{H}(\mathrm{OX}^{-x\varepsilon}) - \bar{H}(\mathrm{OX})]$ is due to the modification of the oxide support upon electron transfer; $(x/2) \cdot [\bar{H}(2\mathrm{H}^{\varepsilon}_{\mathrm{spillover}} - \bar{H}(\mathrm{H_2})]$ corresponds to the formation of hydrogen spillover; and $I_3 - I_i$ corresponds to the modification of the metal–support interaction consecutive to it.

Theoretically, one might further subdi-

vide $\Delta\bar{H}_d$ into $\Delta\bar{H}_a$ and ΔH_b in the manner shown in the thermodynamic cycle; $\Delta\bar{H}_a$ would then be the enthalpy of H_2 dissociation by platinum supported on the transition metal oxide, but it is important to realize that this treatment cannot separate $\Delta\bar{H}_a$ from $\Delta\bar{H}_b$, i.e., from the effect of further interaction of dissociated hydrogen with the surface of the oxide. Remember that x is the uptake per mole oxide, (OX). In the equation above, we chose to express all enthalpy changes per mole H_2.

In order to obtain *separately* $\Delta\bar{H}_i(H_2)$ and $\Delta\bar{H}_d$, we must find a way to estimate $\Delta\bar{H}_i(H_2)$ as defined by Eq. (8). This has been achieved by using a statistical thermodynamics treatment developed in Ref. (*2*), from which Table 1 has been taken. The main principles of this treatment have been recalled in the Introduction. The final equation which applies is

$$\ln A_g = \frac{E_o - E_v}{RT}[1 - \zeta(1-\alpha)^{\zeta-1}] + \zeta(1-\alpha)^{\zeta-1}\frac{\Delta\bar{H}}{RT} + \ln\frac{\alpha}{1-\alpha} - \ln[1 + bX_{om}^{\zeta-1}(1-\alpha)^{\zeta-1}], \quad (10)$$

where α is the ratio of the occupational probability per interstitial lattice site X_o to the maximum occupational probability X_{om}. X_{om} depends on the lattice of interstitial sites which can be occupied by the guest hydrogen,

$$\alpha = X_o/X_{om} = x/N_m, \quad (11)$$

b and ζ are defined as

$$\zeta = ZX_{om}/(1 - X_{om}) \quad (12)$$

$$b = (1 - X_{om})X_{om}^{-\zeta}, \quad (13)$$

where Z is the coordination number of an interstitial site. $(E_o - E_v)$ is the difference in energy between occupied and vacant sites, expressed per gram atom H. The parameters $\Delta\bar{H} = \frac{1}{2}\Delta\bar{H}_i(H_2)$ and $(E_o - E_v)$ in Eq. (10) are optimized in order to fit the experimental isotherm, namely $\ln A_g$ (Eq. (5)) plotted vs α (Eq. (11)). Generally, more than one interstitial lattice gives a good fit, as shown in Table 4.

At this stage it is worth outlining that the interstitial lattice is not a real lattice in the sense that it is not supposed to match the crystal lattice of the host oxide (*2*). The interstitial lattice indicates solely the *neighboring relationships* between interstitial sites which allow one to fill these sites, in a way mimicking the insertion or intercalation process at equilibrium between the gas phase and the solid.

It is, therefore, not surprising that several "interstitial lattices" may yield reasonable fits between "theoretical" and experimental isotherms. Since ζ is the number which characterizes the interstitial lattices, it may be suggested that any lattice with $2.218 \leq \zeta \leq 2.658$ could be used for $H_{2.85}VMoO_{5.5}$.

The numerical values of $\Delta\bar{H}_i(H_2)$, $2(E_o - E_v)(H_2)$, $\Delta\bar{H}_d(H_2)$, and the characteristic

TABLE 4

Best Fitting $\Delta\bar{H}_i(H_2)$, $(E_o - E_v)(H_2)$[a]

Lattice	$-\Delta\bar{H}_i(H_2)$	$-(E_o - E_v)(H_2)$	$-\Delta\bar{H}_d(H_2)$	X_{om}	ζ	Z
Cubic	12.96	14.94	17.54	0.308	2.658	6
Square	12.42	15.22	18.08	0.363	2.274	4
FCC	11.62	14.64	18.88	0.156	2.218	12
Average	12.3 ± 6%	14.9 ± 2%	18.2 ± 4%			

Note. ζ, Z and X_{om}, the maximum occupational probability, are characteristics of the "interstitial" lattice. $\Delta\bar{H}_d(H_2)$ is obtained by difference, using Eq. (7).

[a] In kcal mol^{-1}, calculated from the intercalation isotherm in Fig. 6 (Eqs. (10) and (12)).

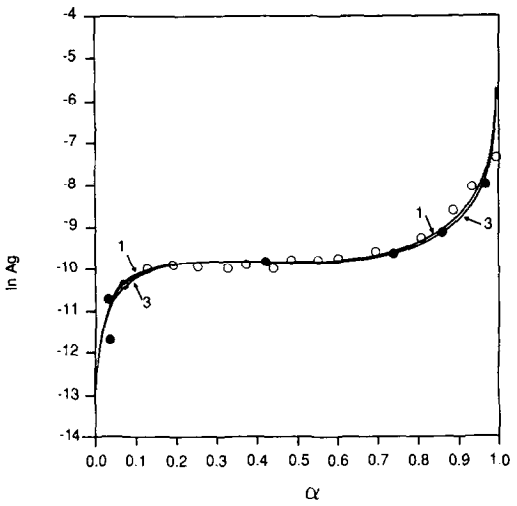

FIG. 6. Calculated isotherms (Eq. (10)) fitting the experimental data shown in Fig. 5. $N'_m = 2.85$. Interstitial lattice: 1, cubic; 2, square (bidimensional); and 3, FCC. 1 and 3 are indicated, 2 is between 1 and 3. Average error on ln A_g: ±0.12 (22 data points). Solid and open circles correspond to data from different isotherms.

values X_{om}, Z, and ζ of the three best fitting interstitial lattices are shown in Table 4. It is worth mentioning that the average error on ln A_g is ±0.12 for the cubic, square, and FCC lattices (Fig. 6). The margin of uncertainty increases very significantly for the triangular, hexagonal, BCC, and linear lattices, indicating poor fits with these lattices. The average $\Delta\overline{H}_i(H_2)$ and $\Delta\overline{H}_d(H_2)$ in Table 4 can be directly compared with the values shown for other bronzes in Table 1. Remembering that $\Delta\overline{H}_{ir}(H_2)$ is −30.5 kcal mol^{-1}, it is obvious that $\Delta\overline{H}_i(H_2)$ in the hydrogen bronze of the mixed $VMoO_{5.5}$ oxide is very similar to that reported for the V_2O_5 bronze. However, $\Delta\overline{H}_d(H_2)$ is 50% larger on Pt supported on $H_{2.85}VMoO_{5.5}$ than on Pt supported on $H_{1.7}MoO_3$. $\Delta\overline{H}_d(H_2)$ is spread over a large range as shown below (in kilocalories per mole):

$$-5.26(H_xWO_3) > -11.4(H_xMoO_3) > -16.9(H_xV_2O_5) > -18.2(H_xVMoO_{5.5}).$$

On the opposite, $\Delta\overline{H}_i$ spreads over a short range of values (in kilocalories per mole):

$$-11.2(H_xWO_3) > -12.2(H_xV_2O_5) \approx -12.4(H_xVMoO_{5.5}) > -13.6(H_xMoO_3).$$

It is worthwhile to emphasize that the results presented in Fig. 4 show that $\Delta\overline{H}_{ir}(H_2)$ is independent of x in $H_xVMoO_{5.5}$. This independence was central to the theory reported in Ref. (*2*), but at the time it was developed the experimental evidence for this constancy was founded in only three experiments. Thus, this is the first important achievement of this contribution.

The second point of interest deals with what could be considered the effect of some kind of strong metal–support interaction (SMSI) on the heat of dissociation of H_2 on Pt, into spilt-over hydrogen (H_s) on the surface of hydrogen bronzes.

In order to explain the large range of $\Delta\overline{H}_d$ we must assemble a puzzle in which several pieces are missing. The situation is summarized in Fig. 7. In Fig. 7b, $\Delta\Phi$ is the difference between the work function (*10*) of the systems Pt, H_xMoO_3 and Pt, $\frac{1}{2}H_2$, OX. $\Delta\Phi$ was measured for the 100 face of a MoO_3 single crystal. In Fig. 7d, E_i represents the energy of ionization of the donor bound level, E_c the energy at the edge of the conduction band, and E_g the gap in $H_{3.3}VMoO_{5.5}$. $E_i - E_c$ and E_g were obtained by plotting the logarithm of the DC conductivity (C) vs $1/T$ for pelletized $H_{3.3}VMoO_{5.5}$, as shown in Fig. 8. The transition between the extrinsic (at low temperature) and intrinsic conductivity (at high temperature) occurs around 400 K. Notice (in Fig. 8) that $VMoO_{5.5}$ itself has a small band gap (E_g = 16.88 kcal) which is about the same as that measured in the high-temperature range for $H_{3.3}VMoO_{5.5}$. In Fig. 7d, the bound donor level E_i must be near the Fermi level of the system. For the reason explained below it was pinned upon $\frac{1}{2}\Delta\overline{H}_d$ obtained for this system. In Fig. 7b, perhaps by coincidence, $\frac{1}{2}\Delta\overline{H}_d$ is exactly equal to the change in the work function. Thus, the change in energy for removing one electron from the Fermi level of the system (Pt, H_s, H_xMoO_3) with respect to the Fermi level of (Pt, $\frac{1}{2}H_2$,

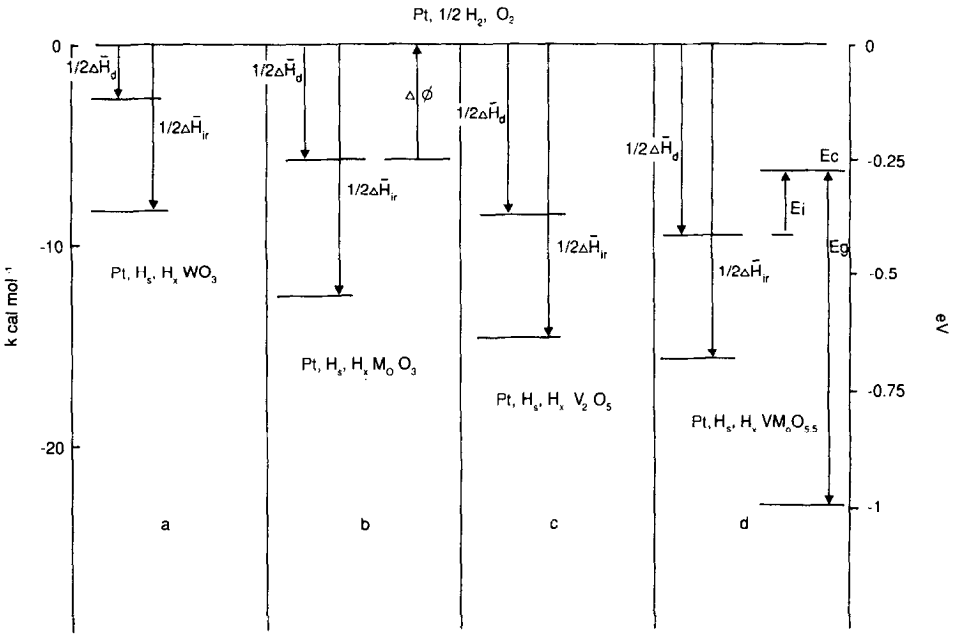

FIG. 7. Energy levels of the (Pt, $H_x^{\varepsilon}OX^{-x\varepsilon}$) systems with respect to the energy level of the Pt, $\frac{1}{2}H_2$, OX corresponding systems. See text.

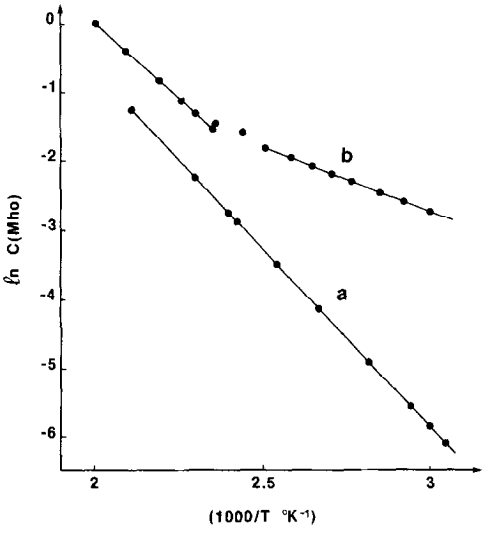

FIG. 8. Logarithm of the conductivity (ln C) vs 1000/T(K) observed for $VMoO_{5.5}$ (a) and $H_{3.4}VMoO_{5.5}$ (b), under 1 atm H_2. In the high-temperature (intrinsic) region, the slope is $-E_g/2k_B$. In the low-temperature region (extrinsic), the slope is $-(E_c - E_i)/k_B$ because of the slight ionization of the uncompensated donors (*14*).

MoO_3) is the same as the value of $\Delta\overline{H}_d$ as defined in Eq. (9). It will be remembered that one of the terms contributing to $\Delta\overline{H}_d$ is, indeed, $\overline{H}(OX^{-x\varepsilon}) - \overline{H}(OX)$.

Now the puzzle starts making sense. Indeed in Fig. 7d the edge of the conduction band is at about the same level as the Fermi level in Fig. 7b. This again may be fortuitous but large differences in the band structure of MoO_3, V_2O_5, and $VMoO_{5.5}$ are not expected in view of their lamellar structure.

In summary, what is suggested here is that the change in the heat of dissociation of H_2 into H_s on Pt particles supported by H bronzes follows the shift of the Fermi level in the (Pt, $H_x^{\varepsilon}OX^{-x\varepsilon}$) system with respect to the Fermi level of the (Pt, $\frac{1}{2}H_2$, OX) system. WO_3 with a ReO_3 structure must have a band structure which differs from that of the lamellar MoO_3, V_2O_5, and $VMoO_{5.5}$ structures; therefore, and as suggested in Fig. 7a, the position of the conduction band edge is not the same in H_xWO_3 as in the other three lamellar bronzes. Indeed $H_{0.4}WO_3$, being a metal, should have its Fermi

level near the edge of the conduction band. This attempt at exploiting the variation of the heat of dissociation of H_2 on supported Pt is no more than a first order approximation and its sole merit is to provide guidelines for further studies.

Irrespective of the validity of the hypothesis underlying Fig. 7, and as far as catalysis is concerned, it is important to emphasize once more that the measurement of the heat of chemisorption of H_2 on a metal supported on an oxide liable to intercalate hydrogen does not provide the heat of dissociation. What is measured is

$$\Delta\bar{H}_{ir}(H_2) = \Delta\bar{H}_i(H_2) + \Delta\bar{H}_d(H_2)$$
$$= \Delta\bar{H}_i(H_2) + \Delta\bar{H}_a(H_2) + \Delta\bar{H}_b(H_2).$$

This remark can be extended to any system such as Ni/TiO_2 or Pt/TiO_2 (anatase) for which an enormous set of references can be quoted (*11*). In agreement with others, Lambert *et al.* (Ref. (*12*)) and references therein) have observed notable H uptake by the TiO_2 host lattice upon reducing at 573 and 773 K while the XRD original pattern of anatase is not modified.

For such systems $\Delta\bar{H}_a$ corresponding to the initial H_2 on platinum is equal to the observed $\Delta\bar{H}_{ir}(H_2)$ minus $[\Delta\bar{H}_i(H_2) + \Delta\bar{H}_b(H_2)]$. Depending on the value of $\Delta\bar{H}_i$ and ΔH_b for the "surface" or "bulk" bronzes formed under these conditions, $\Delta\bar{H}_a(H_2)$ may differ appreciably from the measured heat of chemisorption, $-\Delta\bar{H}_{ir}(H_2)$. However, and in agreement with Sen *et al.* (*13*), $\Delta\bar{H}_{ir}(H_2)$ is not a function of the dispersion of the platinum.

ACKNOWLEDGMENTS

The support of PRF Grant 20472-AC5 is gratefully acknowledged. X. Lin thanks the Laboratory for Surface Studies of the University of Wisconsin-Milwaukee for a research assistantship.

REFERENCES

1. For general review on spillover, see "Spillover of Adsorbed Species" (G. M. Pajonk, S. J. Teichner, and J. E. Germain, Eds.). Elsevier, Amsterdam, 1983.
2. Fripiat, J. J., and Lambert, J. F., *J. Phys. Chem.*, in press.
3. Ancion, C., Marcq, J. P., Poncelet, G., Keravis, D., Gatineau, L., and Fripiat, J. J., *C. R. Acad. Sci. Ser. 2* **296,** 1509 (1983).
4. Tinet, D., Ancion, C., Poncelet, G., and Fripiat, J. J., *J. Chim. Phys.* **83,** 809 (1987).
5. Lin, Xuehao, Lambert, J. F., Millman, W. S., and Fripiat, J. J., *Catal. Lett.*, submitted for publication.
6. Ancion, C., Etude des bronzes d'hydrogene de l'oxyde mixte $VMoO_{5.5}$, Ph.D. thesis, Université Catholique, Louvain-la-Neuve, Belgium, 1986.
7. Ancion, C., Poncelet, G., and Fripiat, J. J., *Mater. Res. Bull.* **20,** 575 (1985).
8. Aston, J. G., and Fritz, J. J., "Thermodynamics and Statistical Thermodynamics," p. 521. Wiley, New York, 1959.
9. Somorjai, G. A., "Principles of Surface Chemistry," p. 249, Table 5.9. Prentice-Hall, 1972.
10. Erre, R., Legay, M. H., and Fripiat, J. J., *Surf. Sci.* **127,** 68 (1983).
11. For a general review on SMSI, see "Metal–Support and Metal–Additive Effects in Catalysis" (B. Imelik, Ed.). Elsevier, Amsterdam/New York, 1982.
12. Lambert, J. F., Poncelet, G., and Fripiat, J. J., *Acta Chim. Hung.* **124,** 121 (1987).
13. Sen, B., Pen Chou, and Vannice, M. A., *J. Catal.* **101,** 517 (1986).
14. Burns, G., "Solid State Physics," p. 321. Academic Press, New York, 1985.